Nuclear Inst. and Methods in Physics Research, A 1052 (2023) 168208

Contents lists available at ScienceDirect

Nuclear Inst. and Methods in Physics Research, A

journal homepage: www.elsevier.com/locate/nima

Radiation tolerant optoelectronics for high energy physics

Jan Troska [a,*], François Vasey [a], Anthony Weidberg [b]

[a] EP Department, CERN, Esplanade des Particules, Geneva, 1211, Switzerland
[b] Physics Department, Oxford University, Denys Wilkinson Building, Oxford, OX1 3RH, United Kingdom

ARTICLE INFO

Keywords:
Optoelectronics
Radiation tolerant
Optical link

ABSTRACT

Optical data transfer has become ubiquitous in the readout and control systems of High Energy Physics Experiments. We review the motivations for this and describe the first large-scale deployments of optical links in the LHC experiments. The current state of the art in the form of the common developments for the LHC upgrade programmes is then summarised. Finally, new technologies and techniques are reviewed and confronted with the needs across the broad spectrum of potential future applications in High Energy Physics.

Contents

* Corresponding author.
E-mail address: jan.troska@cern.ch (J. Troska).

https://doi.org/10.1016/j.nima.2023.168208
Received 25 May 2022; Received in revised form 6 December 2022; Accepted 17 February 2023
Available online 29 March 2023
0168-9002/© 2023 The Author(s). Published by Elsevier B.V. This is an open access article under the CC BY license (http://creativecommons.org/licenses/by/4.0/).

1. Introduction

High Energy Physics (HEP) experiments generate large amounts of data that must be transferred from the detector elements placed in the vicinity of the particle collisions (frontend) to the off-detector control rooms (back-end). At the same time typically smaller amounts of timing and control must be transmitted in the opposite direction. Optical data transmission systems with their potentially very high bandwidths are very attractive for these applications compared to more traditional copper signal cables. Further advantages of optical fibres compared to copper cables are: lower size and mass; lower power; immunity to electro-magnetic interference; and the fact that the electrical isolation provided can alleviate grounding issues in the overall system.

Compared to the telecom and datacom industries that drive the very rapid performance evolution of optical data transmission systems, applications in HEP experiments often have unusual constraints for the on-detector systems. In general they must be sufficiently radiation tolerant and possibly also be non-magnetic, which often requires customisation and application-specific qualification procedures. In addition, HEP applications often require placing optoelectronics in inaccessible locations (such as inside trackers at collider detectors) where they are typically expected to operate for nominal lifetimes of greater than 10 years. While there has been considerable progress on improving reliability for commercial systems, very careful reliability studies remain essential for HEP applications.

The radiation level expected for the optoelectronics installed in LHC experiments and their upgrades has been increasing over time. The typical radiation levels used for the current ATLAS and CMS trackers and the specifications for the LHC phase 1 and phase 2 upgrades are shown in Table 1. Even higher radiation levels are expected for a future 100 TeV hadron collider (e.g. FCC pp) and indicative radiation levels are also given in Table 1.

This review article is structured as follows: Section 2 provides an overview of optical link deployments in HEP experiments from the 1990s up to the LHC experiments. These deployments are characterised by their diversity and after reflection by the various groups that had developed their detector-specific solutions it was realised that a more effective strategy would be to have a common project to develop a 'one-size fits all' module for the optoelectronics for the LHC upgrade programme. This work is summarised in Section 3. We review the R&D for future systems that has already started in Section 4, with a focus on Silicon Photonics before concluding in Section 5.

2. Historical review of optical link deployments in HEP

The first application of optical links in an HEP experiment did not have any requirements on radiation tolerance but developed confidence in the use of this relatively new technology. The first use of optical links in an HEP experiment with a large radiation dose and hadron fluence was the CDF experiment. However, what follows focuses on the applications in the initially-installed LHC detectors. The much higher data rates along with the large increase in channel counts in the LHC detectors compared to previous experiments meant that optical links were adopted for data transfer throughout all LHC experiments. Selected examples will be used to illustrate the large variety of optical link technologies deployed in the LHC experiments. A brief discussion of some of the lessons learned will conclude this section.

2.1. Pre LHC experiments

2.1.1. SLD

The first large HEP experiment to make extensive use of optical links was SLD [1], upgraded in 1996. For this application with very low radiation levels commercial transmitters and receivers were used at a data rate of 960 Mbps over standard commercial optical fibres. This first successful deployment of optical data transmission technology opened the door for what follows.

Table 1
Year of commissioning, approximate number of links and indicative radiation levels for different detectors. The radiation levels for the current ATLAS and CMS detectors refer to the strip trackers. The radiation levels for the LHC phase 1 (phase 2) upgrade refer to calorimeters (trackers). The estimated radiation levels for FCC pp come from a simple scaling of primary particle fluences and expected integrated luminosity compared to HiLumi-LHC [2].

Detector	Year	Channel Count	Dose (kGy(Si))	Fluence Neutron (n_{eq} 1/cm^2)	Fluence Hadron (h 1/cm^2)
SLD	1996	<100	–	–	–
CDF	2004	600	2	1.3×10^{13}	–
LHC 0	2007	200k	100	1×10^{14}	1×10^{14}
LHC Phase 1 upgrade	2020	80k	10	5×10^{14}	
LHC Phase 2 upgrade	2026	200k	1000	1×10^{15}	1×10^{15}
FCC (pp)	2050	TBC	2×10^{4}	3×10^{16}	3×10^{16}

2.1.2. CDF

The first large scale use of optical links in an HEP experiment with high radiation levels was CDF at the Tevatron. CDF used approximately 600 optical links for the readout of the run II tracker [3] from 2001 to 2011. The links were based on Edge Emitting Lasers (EELs) and multimode fibre operating at 1550 nm. The fibre was standard commercial germanium doped Graded Index (GRIN) fibre which had sufficient radiation tolerance. The EEL and the photodiodes were commercially-available InGaAsP/InP 12-way array devices that were custom-packaged to fit the application. The front-end devices were irradiated to a fluence of 1.3×10^{13} (1MeVn$_{eq}$)/cm^2 and the degradation in optical output was acceptable. The links were used successfully in CDF despite multiple problems caused by bad electrical connections (which could be fixed) and some Transmitter (TX) failures that could be recovered by adjusting power supply settings to tune the TX unit light output [4].

2.2. Original LHC experiments

The massive deployment of optical data transmission systems in the LHC experiments was made possible because the basic link technology had reached a sufficient level of maturity. The CERN Detector Research and Development Committee (DRDC), set up in 1990 and later succeeded by the LHC Committee (LHCC), spear-headed the development by setting up its so-called RD-23 initiative for *Optoelectronic analogue signal transfer for LHC detectors* [5] in 1991. Since not all experiments chose analogue readout, a need to develop customised solutions for individual detector systems emerged, leading to a wide range of choices of final link implementations. These implementations fall into two broad categories, analogue and digital optical links, with the CMS tracker favouring the former development path and ATLAS the latter. The then unprecedented radiation levels predicted for the innermost detector layers and the uncertainty in radiation tolerance of optical data transmission components meant that the R&D efforts were essentially concentrated in the Trackers and Calorimeters of ATLAS and CMS. Developments for the outer detectors of ATLAS and CMS as well as those for ALICE and LHCb followed much later, building on what had been learned by the early adopters.

The overall number of optical links deployed in the LHC experiments is summarised in Table 2. We will now describe selected details of the developments for various LHC Experiment sub-detectors.

2.2.1. Front-end transmitters

Whereas the ATLAS SCT chose binary readout early on and pursued a digital optical link development strategy, the CMS tracker chose to use analogue readout and pursued the RD-23 development. Digital links were thought early on to be able to be based on directly-modulated laser diodes. Vertical Cavity Surface Emitting Lasers (VCSELs) were in their infancy at the start of LHC-driven R&D and although they showed

Table 2
Number of optical links in LHC detector systems.

Experiment	Sub-detector	Number of links
ATLAS	Pixels	4116
	SCT	12264
	TRT	768
	Liquid Argon	1524
CMS	Pixels	2000
	Tracker	40000
	ECAL	12000
LHCb	all	3068
ALICE	all	500

promise as a low-power, low-cost solution there was limited information about their reliability. By contrast, LED developments were more mature and the fact that excellent reliability data (see for example [6]) were available initially made the use of LEDs more attractive. However, the radiation tolerance of LEDs was measured to be very marginal [7] for use at LHC. VCSELs were an attractive option because they were shown to have excellent radiation tolerance [7], which led to VCSELs being adopted for use in ATLAS. The remaining reliability concerns were addressed by different strategies:

- Redundant links were used for the SCT [8].
- Pixel optical links were moved to a more accessible location which allowed for the possibility of replacements.
- The Liquid Argon calorimeter used VCSELs in a nominally hermetic package.

All ATLAS systems used AlGaAs VCSELs operating at 850 nm with multimode fibre and readout speeds ranging from 40 Mb/s to 1.6 Gb/s. LHCb also used a single type of oxide-confined 850 nm AlGaAs VCSEL for all systems, and ALICE (with the exception of the pixel detector) also chose a single type of VCSEL in a commercial Transceiver package. There were two main families of radiation tolerant VCSEL driver ASICs used for all custom links (i.e. excluding the ALICE commercial transceivers): the 40 Mb/s-capable VDC [9] designed initially for the ATLAS SCT and then adapted for the ATLAS Pixels; and the 1.6 Gb/s GOL [10] or GLink[1] used by the VCSEL-based links for the TRT and Liquid Argon detectors.

At the early stage of LHC detector R&D, optical modulators were considered for the analogue readout of tracking detectors. Analogue readout was an attractive option for minimising on-detector power and complexity of on-detector radiation tolerant electronics as well as achieving the best signal to noise ratio. Modulator-based optical links were considered a promising technology for the readout of analogue data. The RD23 collaboration studied the functionality and radiation tolerance of modulators [11]. The most promising technology was Multiple Quantum Well (MQW) reflective modulators using the InGaAs/InP material system and good performance and satisfactory radiation tolerance was demonstrated. However, the costs and risks of implementing this technology on a large scale turned out to be significantly larger than the alternative option based on directly modulated edge-emitting diode lasers [12]. In 1997, the CMS tracker opted for a directly-modulated laser-based optical readout. InGaAsP Edge Emitting Lasers (EEL) operating at 1310 nm were chosen over VCSELs for their linearity for the analogue links where data from 256 silicon microstrips were time-multiplexed at a rate of 40 MS/s with an 8-bit-equivalent analogue resolution. A radiation tolerant analogue three-channel linear laser driver array ASIC [13] was designed for this application. The same edge-emitting laser was subsequently adopted by the CMS ECAL for their readout systems, driven by the GOL ASIC at 800 Mb/s, as well as by the control systems of the CMS Tracker, Pixels, ECAL, and Muon RPC systems.

[1] Agilent Technologies HDMP1022/1024.

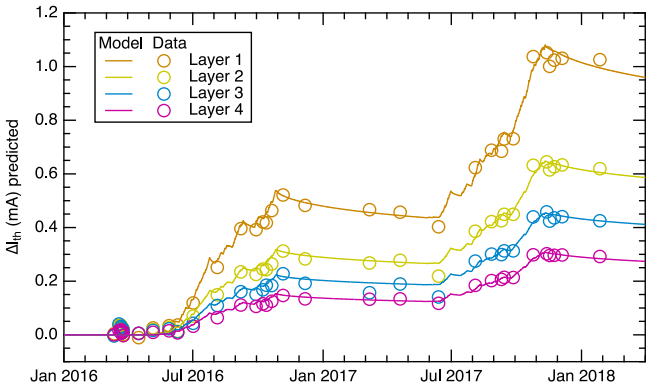

Fig. 1. Change of laser threshold as a function of time compared to simulation for CMS Tracker Inner Barrel layers.

The radiation tolerance of the VCSELs was studied using a variety of beam types and energies [14]. While there was significant radiation damage in terms of an increase in laser threshold current and a decrease in slope efficiency observed immediately after the irradiation, subsequent operation of the devices showed almost complete recovery, so that the radiation damage expected over the LHC lifetime was very small. The expected good radiation tolerance was later verified from in-situ measurements [15] after two LHC runs compared to calculations based on radiation tests before the LHC start-up. Extensive radiation damage studies of EELs were performed and demonstrated that acceptable performance could be obtained up to the maximum expected fluence of 2×10^{14} particles/cm^2 [16]. Very detailed reliability studies of the on-detector optoelectronics using accelerated ageing studies were also carried out. Due to the analogue nature of the CMS Tracker optical links it has been possible to measure radiation damage in-situ during routine operation. The increase in laser threshold for the CMS Tracker Inner Barrel (TIB) [17] during LHC Run 2 shows good agreement with simulation as shown in Fig. 1.

2.2.2. Front-end receivers

All receivers were based on *p-i-n* photodiodes. The ATLAS SCT used silicon photodiodes coupled to a custom receiver ASIC (DORIC [9]) to receive the 40 Mb/s bi-phase mark encoded data and extract the 40 MHz clock. The CMS Tracker used InGaAs photodiodes and a custom receiver ASIC (Rx40 [18]) for its 80 Mb/s digital control link.

The silicon photodiodes used in ATLAS had excellent radiation tolerance and the response was sufficiently fast for the low operating speed [19]. The in-situ analysis of radiation-induced responsivity degradation in the ATLAS inner SCT barrel as a function of integrated luminosity (see Fig. 2) confirmed the earlier predicted result. The radiation tolerance of InGaAs photodiodes was extensively studied by CMS [20]. The radiation-induced decrease in responsivity was mitigated at the system level by supplying sufficient optical power from the back-end. The large measured increase in leakage current was mitigated by designing the Rx40 to be tolerant to large DC currents.

2.2.3. Front-end packaging

Commercially-available optical packaging solutions available at the time of the development of the optical links for the LHC experiments were generally considered to be too bulky to be used in the detector front-ends. This lead all link developments to pursue different packaging solutions. In addition, every application aimed to use a specific combination of transmitter(s) and receiver(s), so there was little possibility for commonality between developments for different detector systems. Overall, these two factors led many detector systems to develop their own custom packages. The ATLAS SCT used a custom opto-package [8] developed by a collaborating institute that contained

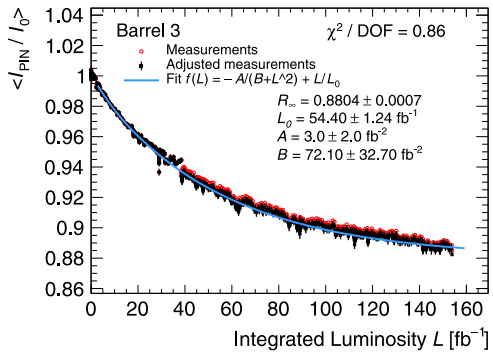

Fig. 2. The relative decrease of photodiode current versus integrated luminosity over the full LHC run 2 for the inner barrel layer of the ATLAS SCT.

two VCSELs and one photodiode coupled to multimode fibres as shown in Fig. 3. Custom packaging for on-detector arrays of VCSELs and photodiodes was also used for the ATLAS pixel system. Here the optical links were at a more accessible location outside the Inner Detector cold volume which allowed for the possibility of replacement.[2]

The optical packages used for the ATLAS Liquid Argon calorimeter contained a commercially-available oxide-confined VCSEL in a hermetic TO can.

In the CMS tracker and ECAL, the EELs were mounted in a semi-custom package, which consists of the laser die attached to a silicon optical submount and fibre-pigtail (see Fig. 4). The photodiodes of the control link were used in a commercial hermetic package with a coaxial pigtail.

2.2.4. Optical fibre

The overall length of the readout and control systems at the LHC was between 50 and 150 m. All VCSEL-based links used multimode optical fibre while the EEL-based links used singlemode optical fibre. The ATLAS SCT used a radiation hard pure silica core Step Index Multi Mode (SIMM) fibre [21]. Although the SIMM fibre had a limited bandwidth, it was sufficient for readout at 40 Mb/s. The ATLAS TRT and Liquid Argon as well as the LHCb systems used standard commercial OM2 Graded Index Multimode (GRIN) fibre. The OM1 fibres used by ALICE were slightly longer at about 200 m. To allow for the higher luminosity in run 2 the bandwidth was increased by replacing their OM1 fibre by OM2[3] fibre.

The EEL-based optical link systems in CMS used standard Single-Mode (SM) fibre which was qualified to be sufficiently radiation tolerant for the application.

2.2.5. Back-end components

Common off-detector optoelectronics based on custom non-hermetically packaged 12-way VCSEL and photodiode arrays were used for ATLAS SCT and Pixels [22]. The off-detector arrays used oxide-implant VCSELs.

Semi-custom off-detector packages were also developed for the analogue links of CMS. The strategy was to replace the digital receiver ASIC in a commercially-available 12-channel receiver with a custom-designed analogue version. This development yielded a very reliable application specific 12-channel receiver [23].

Both LHCb and ALICE used commercially-available receivers on their back-end boards. In the case of LHCb it was a 12-channel receiver and in ALICE it was an SFF-type single channel transceiver.

[2] For the initial operation of ATLAS the pixel optical links were located inside the cold volume of the Inner Detector. This created difficulties with the operation of some VCSELs at low temperatures and heaters were required. In addition there were concerns about the VCSEL failure rate. Therefore in the first long shutdown (LS1) the optical links were moved to a more accessible location outside the Inner Detector cold volume.

[3] OM1 (OM2) fibre has a minimum bandwidth of 200 (500) MHz.km.

2.2.6. Reliability issues

At end of LHC Run 1 in 2014, the fraction of dark ATLAS SCT uplinks forced to use redundancy was 1.6% [8], mainly due to the failure of the on-detector VCSELs. As this number stabilised over time it was ascribed to "infant mortality" in what turned out to be a rather reliable deployment. The ATLAS SCT on-detector opto-packages used early-generation proton-implant VCSELs as there was better reliability data for these than the newer (faster) oxide-implant VCSELs. The attempt to eliminate infant mortality by burn-in was not successful because of the limited temperature 60 °C that could be applied to VCSELs in their customised opto-package. However, a very large rate of failures was observed for the off-detector VCSEL arrays [24]. Studies using Scanning Transmission Electron Microscopy (STEM) of failed VCSELs showed damage propagating to the active Multi Quantum Well (MQW) region that was demonstrated to be due to humidity. The VCSELs were operating in normal humidity conditions in the counting room and these arrays were only designed to be operated at very low humidity inside hermetically sealed packages. The arrays were replaced with VCSELs that used dielectric barriers to prevent humidity damage. Subsequently, a very low rate of failures was observed and after Finite Element Analysis (FEA) was attributed to the strain induced by differential Coefficient of Thermal Expansion (CTE) in the VCSEL and the glue. This shows how the details of the packaging can affect the reliability of the VCSELs. The ATLAS SCT back-end system also used commercially-available VCSELs packaged in a commercial housing which had excellent reliability after a very few cases of infant mortality. There were concerns about the long-term reliability of the pixel optoelectronics because of the problems seen with the SCT and Pixel off-detector systems. Therefore as a precautionary principle, the entire pixel on-detector optical readout was replaced in LHC Long Shutdown 1 using VCSEL arrays that had excellent humidity protection [25]. A link failure rate of about 1% was found in the ATLAS Liquid Argon system and attributed to VCSEL device failure [24]. There is a suspicion that some TO cans containing the VCSELs were damaged in assembly allowing humidity to reach the VCSELs. A strong correlation between VCSEL failures and narrow optical spectral widths was observed. This was very important because it allowed a prediction of which devices were going to fail and thus allowed TX channels with unusually narrow optical spectral widths to be replaced at a convenient time for access. After replacement of all VCSELs identified by their narrow output spectra, no subsequent failures were observed [24].

There was a low rate of VCSEL failures in LHCb where the installed location allowed failed VCSELs to be replaced. As an example, in a typical run at the end of 2012 there were less than 1% dead channels due to failed VCSELs [26] in the LHCb Outer Tracker (OT).

The EEL-based system in CMS had exceptional reliability. At the end of Run 1, a failure ratio of less than 0.1% had been registered.

2.2.7. Lessons learned

Many lessons were learned from the production and operation of optical links for the initial, as built LHC experiments [27]. Some of the key aspects are:

- Avoid diversity of solutions and try to use one system for all experiments. This will reduce the large development costs and result in more reliable systems as more effort will be available for rigorous testing.
- For cost reasons, use digital links operating at the highest possible datarate so as to use all the available fibre bandwidth.
- Use Commercial Off-The-Shelf (COTS) off-detector components.
- Rigorous quality control tests must be performed to take into account realistic operating conditions. If the links are being used in different conditions by different experiments then the experiments must contribute to QA as appropriate to their particular conditions.

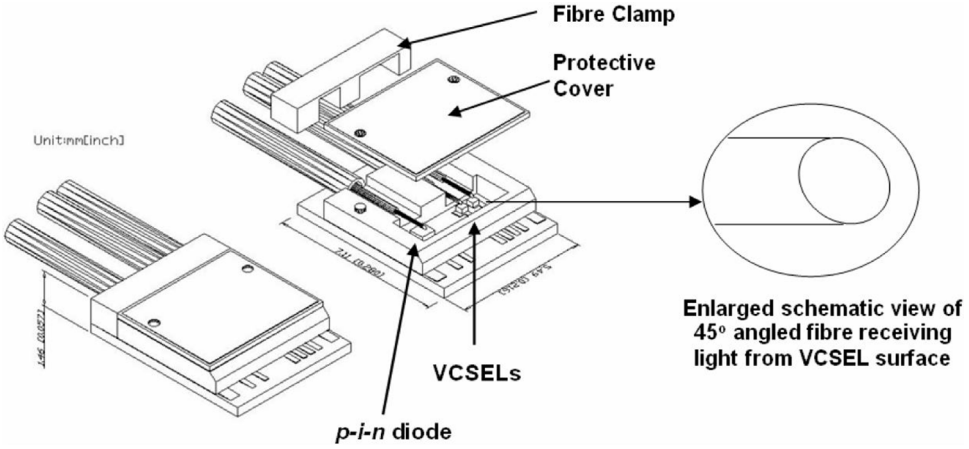

Fig. 3. The ATLAS SCT opto-package showing the 45° fibres coupling to the VCSELs and the photodiode. The overall dimensions are $11.2 \times 5.49 \times 1.46$ mm^3.

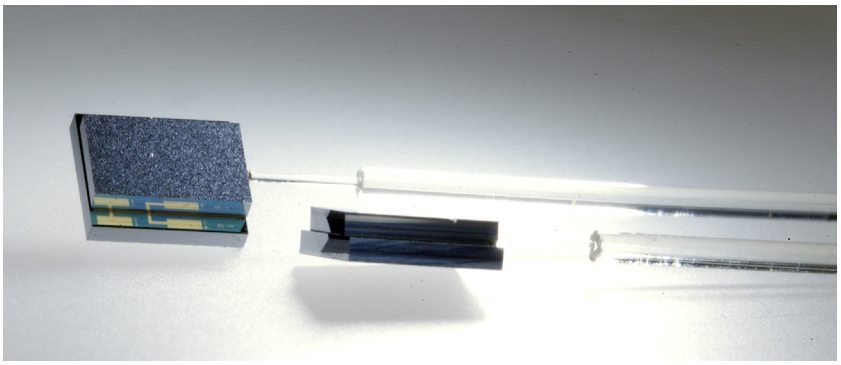

Fig. 4. The custom laser package containing one fibre-coupled EEL used in the CMS tracker and ECAL optical links. The overall dimensions are $4.5 \times 4 \times 1.35$ mm^3.

- The measured in-situ radiation damage observed during LHC operation is in reasonable agreement with the expectations from irradiation studies. The in-situ Single Effect Upset (SEU) rates are harder to extrapolate from irradiation studies but are broadly in agreement with expectations [15].

3. State of the art (phase 1 and phase 2 upgrades of the LHC experiments

3.1. LHC upgrades and common projects

At the time of writing this article, the optical links described in Section 2 have been successfully operating in LHC for over 10 years. During two complete physics runs, several billion operating device-hours have been accumulated by the experiments, demonstrating the suitability and robustness of optoelectronics in the LHC application.

In 2008, at the same time as the LHC machine was started, a number of R&D projects were initiated at CERN to re-group dispersed efforts in the community and to develop in common a set of electronic functionalities to service the future upgrades of the experiments. These included ASIC building blocks in advanced CMOS technologies, DC-DC converters for point-of-load power distribution [28], and optical links [29]. This initiative seeded the development of the electronics which is currently being installed or produced for two phases of upgrades of the LHC experiments: phase I upgrades (2019–21) and phase II upgrades (HiLumi or HL-LHC, 2026–28). Optoelectronics was covered by the Versatile Link and Versatile Link + projects [30,31] while the GBT and LpGBT projects [32,33] developed the corresponding aggregating and high speed serialising/deserialising electronics. This combination of electronics and optoelectronics developed in common by the community under the leadership of CERN led to the general adoption of a single turnkey solution for the transfer of readout and control data in the to-be-upgraded detectors. In practical terms, it resulted in concentrating the community effort on one single radiation-hard link transferring data for DAQ, Trigger, Control, Monitoring and Timing functions, as schematically sketched in Fig. 5.

In this section, we will focus on the Versatile Link (VL) and Versatile Link + (VL+) projects which are representative of state-of-the-art link technologies for HEP.

3.2. The Versatile Link projects (VL and VL+)

The VL and VL+ projects were launched to meet the needs of the detectors upgrading during LHC Long Shutdowns LS2 (Phase I 2019–21) and LS3 (Phase II 2026–28) respectively. Their specifications matched the performance offered by two generations of serializer/deserializer ASICs developed for the same applications: GBTx and lpGBT respectively. Table 3 compares the most salient characteristics of the two systems.

The VL project was driven by a generalist vision: (i) a bidirectional front-end transceiver implemented as a customised module based on the well defined standard SFP+ format [34]; (ii) a choice of one or two Commercial off The Shelf (COTS) Transmitter Optical Sub Assemblies (TOSA) and/or one customised Receiver Optical Sub Assembly (ROSA) enabling compatibility with the two installed legacy MM and SM fibre plants; (iii) a relatively modest radiation resistance requirement matching the needs of mainly ALICE and LHCb detectors; and iv) a pair of full custom digital laser driver (GBLD) and receiver (GBTIA) ASICs. This vision offered a single technological evolution to the multiple systems that were in place in the experiments since the beginning of LHC, with some level of backward compatibility with the legacy cabling plant (SM or MM) if required. Also, its optical power budget was robust enough

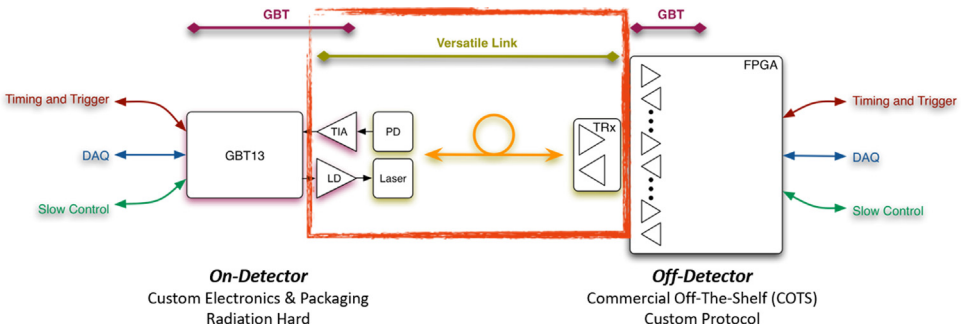

Fig. 5. Common (opto)electronics developed for the transfer of readout, trigger, timing and control data between experiments front- (left) and back-ends (right) in the framework of the GBT and Versatile Link projects.

Table 3
Characteristics of the VL and VL+ systems. Data transmission directions are denoted *Up* (for up-stream) for data transmitted from the detector to the control room and *Down* (for down-stream) for the reverse direction.

	Versatile Link	Versatile Link+
Upgrade phase	Phase I	Phase II
Optical Mode	Single- and multi-mode	Multi-mode
Flavours	1Tx+1Rx, 2Tx	up to 4Tx, +1Rx
Radiation Resistance	Up to Calorimeter grade	Up to Tracker grade
Form factor	SFP+	Custom miniature
Data rate	Up/Down: 5 Gb/s	Up: 5/10 Gb/s, Down: 2.5 Gb/s

and the radiation induced penalties were low enough that standard COTS transceivers could be used at the back-end of the system. The experiments were thus left free to select the implementation of their fibre plant and of their back-end transceiver modules while the VL project only developed and produced the VTRx front-end transceiver. For those detectors upgrading their links, the only migration imposed by the VL system was the digital one, as the developed VTRx module did not support analogue modulation formats such as used in the CMS Tracker (see 2.2.1). This however did not cause a problem since all LHC detectors opted for digital readout for their upgrades.

In contrast to the rather generalist VL project vision, the next generation VL+ radiation tolerant link focused on the more demanding constraints of the ATLAS and CMS trackers and calorimeters representing the majority of the phase II upgrade needs. Extreme radiation resistance, slim footprint and low power dissipation were new constraints that pushed the development in the direction of a finely tuned and customised system. This explains in particular why the VL+ up- and down-links were designed to have asymmetric data-rates and a different number of channels: a single 2.5 Gb/s down-link minimises power and enables improved Single Event Effect (SEE) robustness of the front-end receiver; while multiple 10 Gb/s up-link channels allow for maximising the transmitter data bandwidth to the back-end. The VL+ development effort focused on a unique full custom multi-mode VTRx+ transceiver based on a 4-channel laser driver array ASIC (LDQ10 [35]), a quad VCSEL array, and a single channel *p-i-n* photodiode connected to a transimpedance amplifier (the GBTIA, already used in the previous generation VTRx module [36]). An optical coupling block precisely aligned to the VCSELs and photodiodes interfaces to a 5-fibre bundle terminated with a multi-channel MT optical connector. Due to the large worst case penalties expected to be induced by radiation and dispersion, the VL+ optical power and dispersion budget is tight. The fibre plant and back-end transceivers must thus be specified to match these constraints and cannot be left open to free choice as was the case with the VL link. The VL+ system thus achieves much higher up-link capacity and better radiation resistance than its VL predecessor, at the expense of a single, customised and tightly specified solution.

3.2.1. The Versatile Transceiver projects (VTRx and VTRx+)

The VTRx and VTRx+ transceivers are shown side by side in Fig. 6. The VTRx module is a low-mass, non-magnetic adaptation of the SFP+ package standard, while the VTRx+ module can be seen as a stripped and customised QSFP transceiver [37] where only the so-called optical engine part is retained. The two generations are separated in time by approximately 7 years, but despite significant differences, both developments had to face similar challenges, in particular the radiation hardness of their electronic and optoelectronic components. While ASICs are full custom developments hardened by design, the laser and photodiodes are commercial parts selected and qualified for operation in the harsh LHC and High Luminosity LHC (HL-LHC) environments. Thus, as the optoelectronics cannot be customised, it is the electronics which must be designed to adapt to the radiation-induced changes in lasers and photodiodes.

Fig. 7 shows the evolution of threshold current and output power of different VCSEL types as a function of particle fluence. As particles damage the crystal lattice, non-radiative recombination centres are created that degrade the light emission efficiency of the device. Mitigation of these effects is achieved by: designing the laser driver with programmable output current offset and gain [35]; selecting lasers with best threshold, efficiency and series resistance characteristics; and by including sufficient margin in the link power budget.

Fig. 8 shows the evolution of responsivity and dark current of different *p-i-n* photodiode types as a function of particle fluence. Here also, defects induced by the impinging particles give rise to leakage paths and decreased responsivity. Different material systems (GaAs or InGaAs) used for the light absorbing volume have very different behaviours, requiring the link system to either tolerate large responsivity drops (GaAs), or the transimpedance amplifier to cope with large leakage currents (InGaAs). The VL and VL+ systems are tolerant to both degradation mechanisms and actually use the same transimpedance amplifer [36]. The VTRx module can host either a multimode GaAs Receiver Optical Assembly (ROSA) or a single mode InGaAs ROSA, while the VTRx+ module exclusively uses an InGaAs *p-i-n* diode to maintain operational margin in the down-link up to the most extreme fluences expected in the HL-LHC applications.

Both laser driver and transimpedance amplifier are full custom designs implementing the mitigation schemes mentioned above. The biasing voltages of the *p-i-n* photodiode (reverse bias) and laser diode (forward bias) are also important parameters to consider. In particular, the compliance voltage of VCSELs can be high due to the elevated

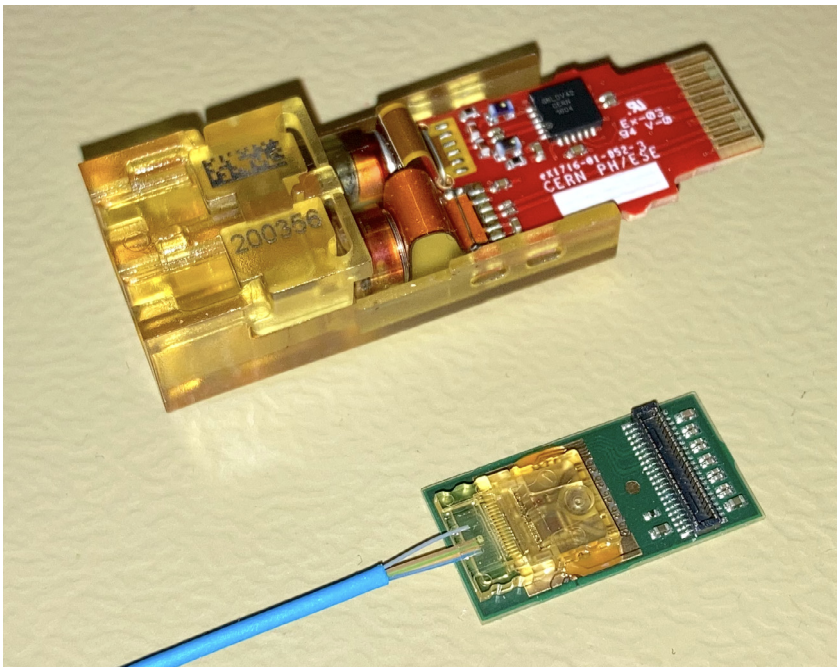

Fig. 6. The two Versatile Transceiver module generations side by side: the two-channel VTRx (top) and the five-channel VTRx+ (bottom). The VTRx measures $45 \times 14.5 \times 10$ mm^3 and the VTRx+ $20 \times 10 \times 2.5$ mm^3.

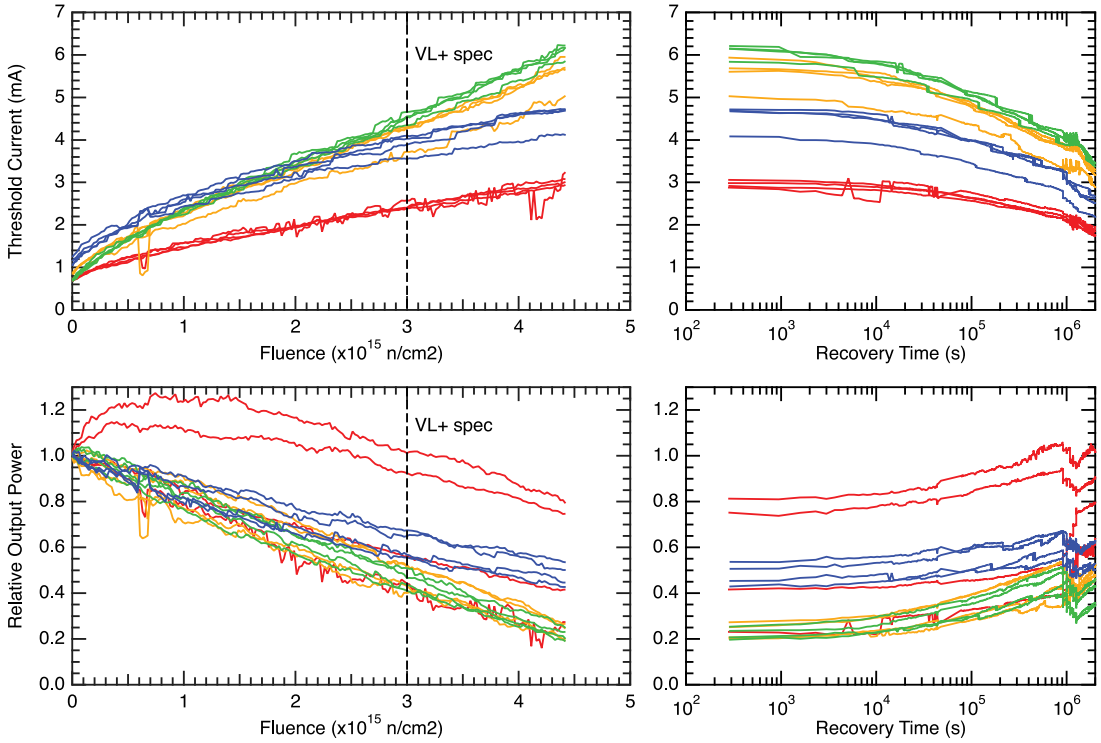

Fig. 7. Threshold current and relative optical output power shifts of different VCSEL types (different colours) as function of neutron fluence (left) and annealing time (right).

series resistance of these devices. Special care must thus be taken when designing VCSEL drivers in advanced CMOS nodes (powered by low supply voltages) that the achievable output voltage complies with VCSEL operating points reaching up to 2.2 V.

Fig. 9 illustrates the performance achieved with the final VTRx+ components. Despite this remarkable resistance, the VTRx+ can unfortunately not be used in the innermost pixel layers or very forward detector regions where accumulated fluences reach or exceed 2 ×

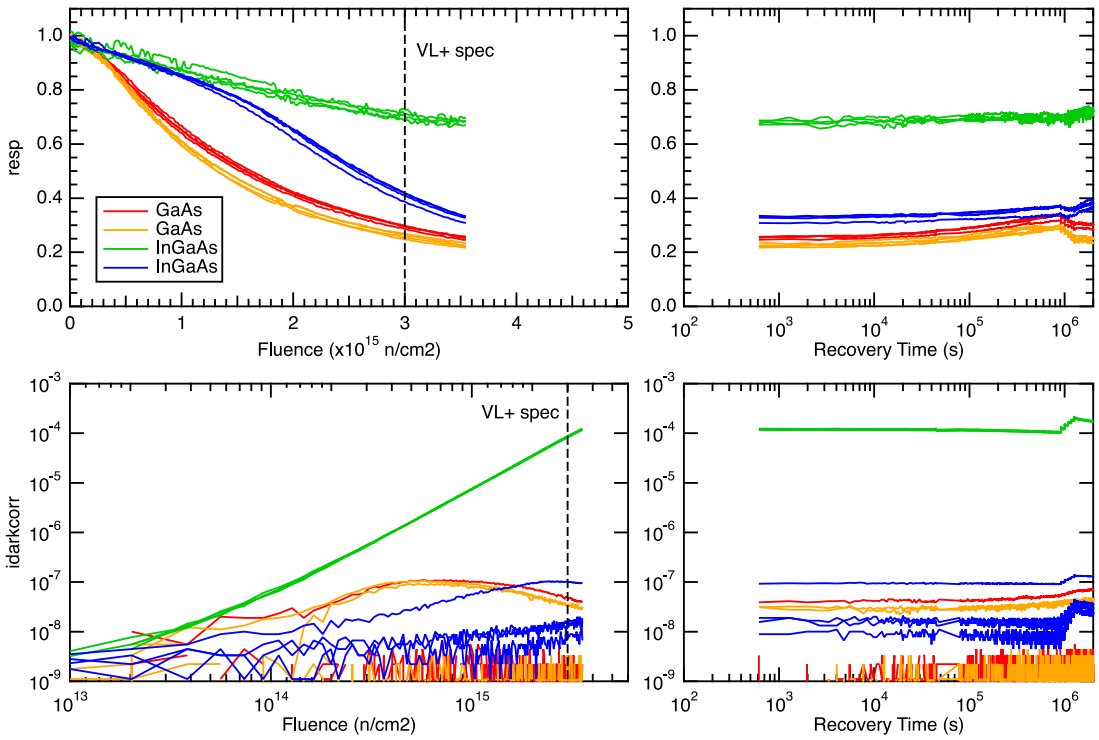

Fig. 8. Relative responsivity and dark current shifts of different *p-i-n* photodiode types (different colours) as function of neutron fluence (left) and annealing time (right).

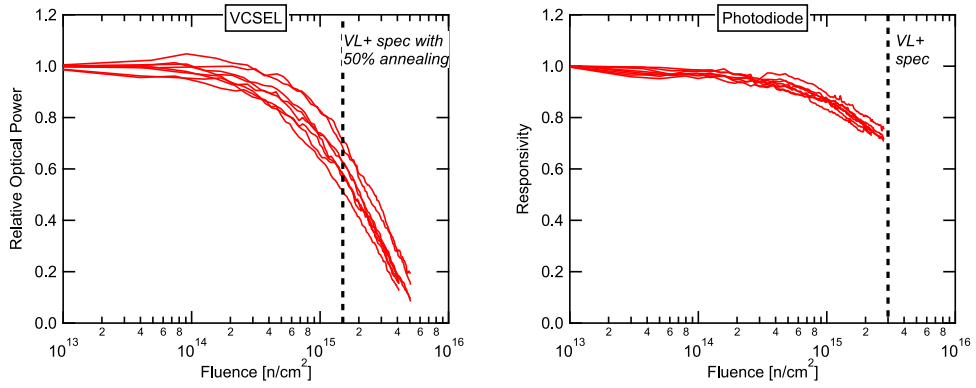

Fig. 9. Performance of VTRx+ transmit (left) and receive (right) path components as a function of neutron fluence during accelerated radiation testing.

10^{15} particles/cm^2. This is likely a hard limit for laser-based transmitters, due to the intrinsic sensitivity of their active layer to displacement damage. Possible solutions for extreme radiation levels are discussed in Section 4.

Designing the custom ASICs and selecting suitable opto components are two necessary and essential parts of transceiver development. However, assembling these components on a PCB and aligning them with the optical coupling elements can be equally challenging, especially if high volume, high yield, high reliability, and low cost requirements are combined. For both VTRx and VTRx+ projects, these steps were partly contracted to industry. CERN designed the PCB and developed the test systems, while the contractor performed volume assembly and production testing. 18'000 VTRx modules were produced in 2016–2019 while 60'000 VTRx+ modules will be produced in 2022–2024. These are significant volumes for a niche application like HEP, necessitating thorough quality assurance and continuous monitoring during production. However, despite all efforts to catch defects and non-compliances, it is impossible to reproduce in the lab all the exact operating conditions in a detector, and early in-the-field failures cannot always be avoided. This was the case in 2021, when the VTRx modules being commissioned in the experiments during LS2 were shown to fail due to outgassing of the ROSAs and re-condensation on the fibre ferrules [38]. Such events can only be mitigated by subjecting ahead of installation time statistically significant numbers of modules to their final operating conditions and observing their long term behaviour, so that recovery or corrective actions can be implemented early on.

3.2.2. *Optical fibre radiation hardness*

Selecting the right optical fibre is crucial to maintaining link performance over its lifetime in a harsh detector environment. The parameters to take into account when assessing fibre suitability are: fibre type (SM or MM), wavelength, data-rate and distance, as well as total ionising dose, dose rate and temperature. Extensive literature exists that describes the radiation hardness properties of optical fibres [39,40]. For the first VL system generation, COTS fibre could be used thanks to the modest radiation levels expected in the final applications [39]. However, for the VL+ system generation, radiation hard fibre has to be used to survive in the most exposed areas of the experiments. This fibre is produced in small batches, and samples from each preform are irradiated to qualify each individual batch. For VL+ systems, more than

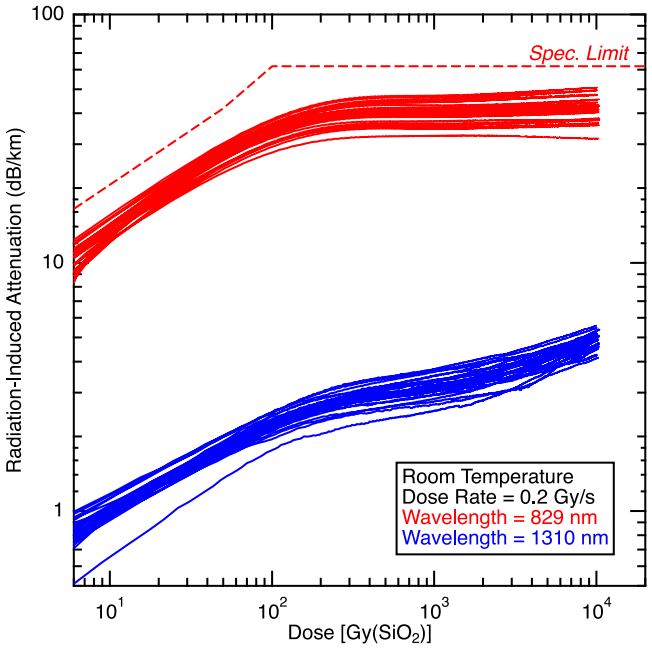

Fig. 10. Radiation induced attenuation in all preforms required for VL+ fibre production.

800 km of rad-hard fibre have been produced and qualified. Fig. 10 illustrates the homogeneity of the radiation resistance results obtained for all tested preforms as part of the fibre qualification programme.

Unfortunately, the bandwidth of the particular rad hard fibre selected for the VL+ system is specified as 500 MHz km. Although there are data to suggest that the as-produced fibre in fact has bandwidths above 2000 MHz km [41], one cannot exclude that even small lengths may cause a dispersion penalty to the system, especially at high datarate. Both radiation-induced attenuation and dispersion penalty must thus be mitigated in radiation hard optical links. For instance, the VL+ optical power budget for the harshest tracker environments (so-called extended grade VL+) allows for up to 6.9 dB of radiation-induced penalty in the down-link and up to 2.3 dB of dispersion-induced penalty in the 10 Gb/s up-link [42]. In future high data-rate applications, dispersion will certainly be one of the critical factors determining the technologies to be selected, as highlighted in the next section.

4. Future evolution (beyond HL-LHC experiments)

Future HEP detector systems will, in all likelihood, generate ever increasing amounts of data as a consequence of both increases in luminosity of the accelerators and the need to acquire additional types of data from the collisions like timing information. This, depending on the accelerator environment, is very likely also to be accompanied by increased levels of radiation. There might also be new applications were other parameters like mass and power consumption become critically important. To face the challenge of meeting these multiple and sometimes conflicting requirements, new technologies being deployed in the telecom and datacom industries could be brought to bear. For instance, in order to increase the throughput of individual fibre links, multi-level signalling technologies like PAM4 [43] might be used, or one could combine multiple datastreams transmitted at different wavelengths through a single optical fibre.

Simply continuing along the incremental development path of directly modulated VCSEL-based links is going to be challenging for several reasons. The first is the potentially extreme levels of radiation that will be encountered in future detectors at, for example, the FCC accelerator. VCSELs cannot survive beyond approximately 3 to 5×10^{15} particles/cm^2 [44] and so an alternative will need to be identified for such applications. The same holds true of other lasers and modulators built on both GaAs and InP platforms [44,45]. A further problem for typical VCSEL-based links is that they use multi-mode fibre which is limited in its Distance-Bandwidth product. This means that as the data-rate increases, so the transmission distance decreases. For example, while commercial 10 Gb/s links can support link lengths of 300 to 400 m that cover the typical needs of HEP experiments, 25 Gb/s links can support link lengths of only 100 to 125 m which is insufficient in many cases.

A very promising new technology is Silicon Photonics (SiPho), which uses mature CMOS ASIC production technology to pattern light-manipulating structures onto SOI wafers. This technology opens the door to custom designed optoelectronics, which could be adapted to the particular set of requirements (data-rate, power, size) of a given application. The industry is also developing new packaging concepts for SiPho technology that offer very interesting possibilities for much tighter integration between the optical link and front-end electronics. These promising approaches are reviewed in more detail in the following sections.

4.1. Promising technologies

4.1.1. Silicon Photonics

The new technology that has garnered the most interest with the HEP community up to now is Silicon Photonics [46]. While it is very difficult to build optical sources in pure silicon due to its indirect bandgap, it is possible to design structures that manipulate light so as to be able to modulate it and create a data transmitter. Two popular modulator structures are ones based on Mach–Zehnder interferometers and ones based on micro-ring resonators. While Mach–Zehnder Modulators (MZMs) are relatively easy to implement and stable to process and temperature variations, they are rather large (mm-scale) devices and generally require driving voltages in excess of 1.5 to 2 V to achieve useful modulation depths. In contrast, Ring Modulators (RMs) are much smaller (5 μm to 10 μm) and require lower driving voltages but due to their resonant nature are much more affected by process and temperature variations to the point of requiring the use of thermal tuning via integrated resistive heaters. Overall, the promise of the highest level of integration and lowest power is offered by RMs, at the expense of having to implement an additional thermal control loop to stabilise their operation.

The key requirement that differs in HEP applications compared to standard applications is radiation tolerance, and it is this aspect that has been studied in significant detail so far in order to assess the suitability of the technology for deployment in future detector systems. Initial studies [47] showed that the basic technology is very resistant to displacement damage but sensitive to ionisation effects. Radiation effects modelling of the devices [44] enabled the design of more radiation tolerant MZM devices [48]. The most recent results show that ongoing foundry process developments have significantly increased the radiation tolerance of standard so-called building block devices that are provided by foundries [49]. It may thus now become possible to use standard building block devices to design application-specific Photonic Integrated Circuits (PICs) that will tolerate MGy levels of radiation, as shown in Fig. 11.

The ability to custom-design application-specific PICs opens up the possibility of tailoring the optical link system to the particular system requirements and means that, for example, Wavelength Division Multiplexing (WDM) could be more easily and widely applied within future detector systems. One outcome of this could be the aggregation of data from multiple front-end ASICs by simply combining them on multiple wavelengths rather than requiring an additional electrical aggregation ASIC, saving design effort, power, space, and cost. For the first time in the field, such customisation at the level of the optical data transmission system is within reach and could lead to different

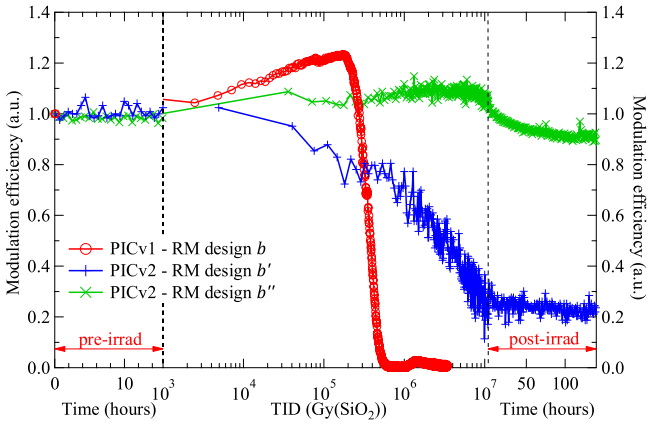

Fig. 11. Effect of radiation on modulation efficiency of three PIC designs showing that tolerance to extreme levels of radiation is possible by careful design.

optimisation choices in future detector readout systems. Fig. 12 shows a prototype SiPho PIC and a possible demonstration system [50]. For ultimate radiation tolerance the optical power source needed for such systems would have to be located in a low-enough radiation area as given by the radiation tolerance of the source.

4.1.2. Advanced modulation schemes

All digital detector readout systems to date have used Non-Return to Zero (NRZ) coding, which is a basic ON-OFF keying method. This is the simplest physical encoding scheme to implement, but it does not maximise the use of the available channel bandwidth. Commercial use of multi-level signalling is becoming more prevalent as a way to increase the use of channel bandwidth. In particular, most recent link standards use Pulse Amplitude Modulation with 4 levels (PAM4). PAM4 encodes 2-bit symbols, thus halving the required channel bandwidth for a given data-rate compared to NRZ at the expense of additional complexity in both transmitter and receiver to generate and detect the four different amplitude levels used. PAM4 coding, due to the multiple signalling levels, has an intrinsically lower signal amplitude and is more susceptible to noise as the levels are closer together. Overall, this means that PAM4 has a worse Signal-to-Noise Ratio (SNR) than NRZ coding, with an SNR penalty of approximately 9.5 dB. For optical communications, this SNR penalty brings additional challenges and the bandwidth vs SNR tradeoff is not the same as it is for electrical signalling. The decision to adopt PAM4 for future HEP data links is therefore still open and will be influenced by the true bandwidth needs as well as the complexity to design and fabricate the system as a whole. Fig. 13 shows an example PAM4 eye diagram from an early prototype radiation tolerant Silicon Photonics transmitter designed at CERN.

4.1.3. Co-packaging

Ever-higher aggregate bandwidths in datacom processors (network switches, for example) are leading to the need to more tightly integrate the Serialiser-Deserialiser (SERDES) and the optical-to-electrical conversion components. Whereas current ASIC generations can still drive the electrical signals over 10 to 15 cm to the front panel where the conversion to optical can take place, this is quickly becoming prohibitive in terms of signal integrity and power dissipation as data-rates increase. The datacom industry's response to this problem is to develop miniaturised optical blocks that can be tightly integrated into the packaging of the ASIC containing the SERDES. Such Co-Packaged Optics (CPO) units are generally agreed in the industry to be the next step, and will lead to the development of new integration technology. This could very effectively be employed in future HEP systems to enable the design of low power, low mass detector modules with optical readout.

4.1.4. Novel fibres

Hollow core fibre [51] is a novel optical fibre design in which the light is guided in air in the micro-structured core of a silica glass optical fibre, an example of which is shown in Fig. 14. The advantage of such a fibre is that the propagation speed increases with guiding in air vs glass resulting in the lowest possible data transfer latency. For HEP applications, such fibres have previously been shown to be very radiation resistant [52], since the typical loss mechanisms introduced by the irradiation of glass are not relevant when the majority of the optical power is guided in air. One major limitation to the wider adoption of this technology has been the difficulty of producing the multiple kilometer lengths typical of standard optical fibre production. New production techniques are actively being developed and are starting to bring the advances required for such fibres to be more readily available and their characteristics are starting to approach those of standard fibres [53]. Once successful, hollow core fibre could become interesting in HEP applications where extreme levels of radiation cannot be avoided along the path of the optical fibres.

4.1.5. Evolution of VCSEL-based systems

Current state of the art HEP fibre systems are all based on VCSELs. We have already shown that there is a limit to the radiation tolerance of such devices, which excludes their use in the most extreme environments. Many HEP systems do not require very high levels of radiation tolerance and it is therefore instructive to consider whether industry developments are moving in the same direction as HEP systems. Current VCSEL developments for 56G and beyond line rates are still based on multimode fibre, which limits the reach of such links due to dispersion. Link length is therefore becoming the key parameter when assessing whether VCSEL-based links have a future in HEP applications with low radiation level requirements. For example, the typical link lengths for LHC experiments are in the range of 60 to 400 m, compared to the maximum reach of 100 m of the 400GBASE-SR4 standard [54] that runs 53.1250 GBd PAM4 signals over multimode fibre. This would limit the areas in which such technology could be applied, making a single development difficult to achieve.

4.2. Optical link system evolution

It is instructive to consider which application requirements drive the optical links specifications: bandwidth, power, and/or radiation tolerance. Different HEP applications will clearly have a different mix of these requirements. Moving from the initial model of link development within HEP where each individual application developed its own specific optical link to the more recent common development has brought with it the need to very carefully consider how best to target the specifications considering the wide range of actual final requirements. Sometimes this has led to design decisions that were necessarily taken early in the process which have later turned out to be over-constraints that have allowed subtle difficulties [38] to appear.

Future common developments might target more than one generic specification for typical use cases in different environments. For example, one might propose a highly-integrated, low power design for lower radiation levels for future very low mass tracking systems; as well as a differently optimised design targeting the highest radiation levels, perhaps at the expense of higher power consumption. Another key consideration is the one of interoperability with commercially available optical link components that can be used in the off-detector back-end electronics. This assumption of being able to use commercial components in the back-end might be challenged by the desire to highly customise the front-end components. As data-rates increase commercial transceiver vendors employ components that become more restrictive in terms of the actual supported data-rates, whereas previous transceiver generations have been much more rate agnostic. This challenges the freedom to choose the exact datarate of an HEP link which then may no longer be able to remain synchronous to the accelerator

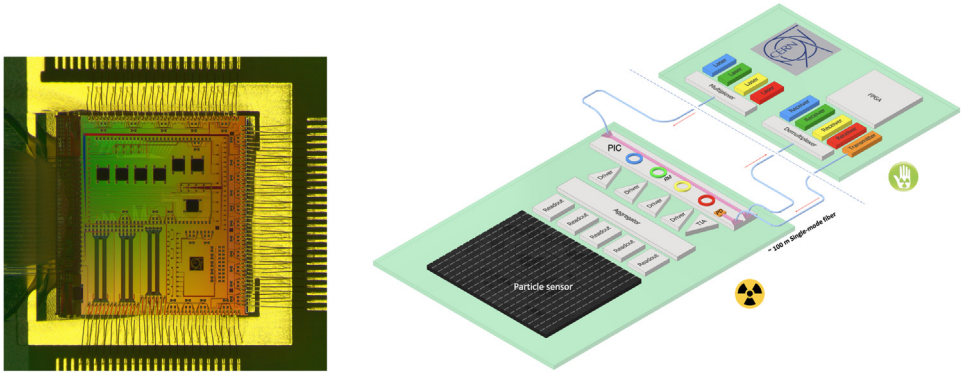

Fig. 12. Photograph of prototype PIC (left) and example Silicon Photonics link (right).

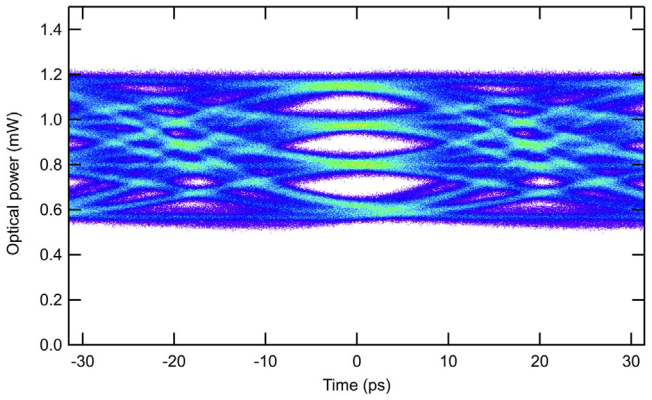

Fig. 13. 25 GBd PAM4 eye diagram from an early prototype silicon radiation tolerant photonics transmitter.

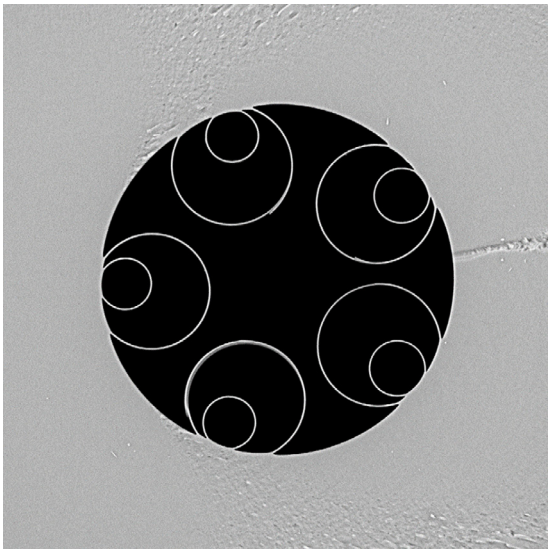

Fig. 14. Photograph of a Hollow core Nested Antiresonant Nodeless (NANF) fibre.

beam frequencies. While this might seem like a detail, it potentially has wide-ranging implications for the entire detector system design. Similar challenges might be valid for other optical link parameters, for example the choice of wavelengths in a WDM system. Current R&D programmes [55,56] are investigating such issues and will provide guidance once completed.

5. Summary and conclusions

The use of optical links in HEP experiments has evolved over the last 30 years from being an exotic technology to the standard one to provide the very high data bandwidth required. The first generations of optical links used a very wide variety of technologies, featuring different wavelengths and different laser and photodiode technologies. While this approach did eventually succeed for the first generation of LHC detectors, many problems had to be faced and it was realised that the multiple developments were very inefficient in resources. Therefore an approach based on common solution(s) was developed for the phase 1 LHC upgrades based on the VTRx package. This approach still allowed for the use of EELs or VCSELs. However, for the tracker phase 2 upgrades for the HL-LHC, much higher radiation levels are expected. As VCSELs show better radiation tolerance than EELs and a more favourable performance/price ratio for HEP experiments, the VTRx+ project was based exclusively on VCSELs. The future R&D directions outlined in this paper are addressing the challenges of very high data rates and increased radiation tolerance that will be required by future HEP applications. The development of silicon photonics is particularly interesting as it offers very attractive customisation and integration possibilities, high data rates and greatly improved radiation tolerance compared to more conventional lasers and photodiodes.

Declaration of competing interest

The authors declare that they have no known competing financial interests or personal relationships that could have appeared to influence the work reported in this paper.

References

[1] K. Abe, Design. and performance of the SLD vertex detector, a 307 mpixel tracking system, Nucl. Instrum. Methods A 400 (1997) 287, http://dx.doi.org/10.1016/S0168-9002(97)01011-5.

[2] A. Abada, et al., FCC-hh: The Hadron collider, Eur. Phys. J. Spec. Top. 228 (2019) 755–1107, http://dx.doi.org/10.1140/epjst/e2019-900087-0.

[3] S. Hou, Radiation hardness of the 1550 nm edge emitting laser for the optical links of the CDF silicon tracker, Nucl. Instrum. Methods A 511 (2013) 66, http://dx.doi.org/10.1016/j.nima.2005.01.058.

[4] T. Aaltonen, Operational experience, improvements, and performance of the CDF run II silicon vertex detector, Nucl. Instrum. Methods A 729 (2013) 153–181, http://dx.doi.org/10.1016/j.nima.2013.07.015.

[5] J.D. Dowell, P.M. Hattersley, R.J. Homer, P. Jovanovic, I. Kenyon, R. Staley, K. Webster, C. Da Via, J. Feyt, P. Nappey, G. Stefanini, B. Dwir, F.K. Reinhart, J. Davies, N. Green, W. Stewart, T. Young, G. Hall, T. Akesson, G. Jarlskog, S. Kröll, R. Nickerson, S. Jaroslawski, Optoelectronic analogue signal transfer for LHC detectors, 1991; 1991 ed., Tech. Rep., CERN, Geneva, 1991, URL https://cds.cern.ch/record/315435.

[6] T. Lutz, M. Ritzer, Reliability and lifetime of LEDs, 2020, URL https://media.osram.info/media/img/osram-dam-2496614//AN006_Reliability_and_lifetime_of_LEDs.pdf.

[7] J. Beringer, et al., Radiation hardness and lifetime studies of LEDs and VCSELs for the optical readout of the ATLAS SCT, Nucl. Instrum. Methods Phys. Res. A 435 (3) (1999) 375–392, http://dx.doi.org/10.1016/S0168-9002(99)00570-7.

[8] A. Abdesselam, et al., The optical links of the ATLAS semiconductor tracker, J. Instrum. 2 (2007) P09003, http://dx.doi.org/10.1088/1748-0221/2/09/P09003.

[9] D. White, J. Dowell, G. Mahout, P. Jovanovic, I. Mandić, A. Weidberg, Radiation hardness studies of the front-end ASICs for the optical links of the ATLAS SemiConductor tracker, Nucl. Instrum. Methods Phys. Res. A 457 (1) (2001) 369–377, http://dx.doi.org/10.1016/S0168-9002(00)00763-4, URL https://www.sciencedirect.com/science/article/pii/S0168900200007634.

[10] P. Moreira, A 1.25 Gbit/s Serializer for LHC data and trigger optical links, in: Proceedings of the Fifth Workshop on Electronics for LHC Experiments, Snowmass, Colorado, USA, 1999, p. 194, URL https://inspirehep.net/literature/513508.

[11] The RD23 Collaboration, Status report on the RD-23 project : Optoelectronic analogue signal transfer for LHC detectors, 1993, URL https://cds.cern.ch/record/291165.

[12] F. Bourgeois, Review of the outcome of two workshops on electronics for LHC experiments, Tech. Rep., CERN, Geneva, 1997, URL https://cds.cern.ch/record/328725.

[13] G. Cervelli, A. Marchioro, P. Moreira, F. Vasey, A Radiation tolerant laser driver array for optical transmission in the LHC experiments, 2001, http://dx.doi.org/10.5170/CERN-2001-005.155, URL https://cds.cern.ch/record/529399.

[14] P. Teng, et al., Radiation hardness and lifetime studies of the VCSELs for the ATLAS SemiConductor tracker, Nucl. Instrum. Methods Phys. Res. A 497 (2) (2003) 294–304, http://dx.doi.org/10.1016/S0168-9002(02)01922-8.

[15] I. Dawson, et al., In situ radiation damage studies of optoelectronics in the ATLAS SemiConductor tracker, J. Instrum. 14 (07) (2019) P07014, http://dx.doi.org/10.1088/1748-0221/14/07/p07014.

[16] K. Gill, R. Grabit, J. Troska, F. Vasey, Radiation hardness qualification of InGaAsP/InP 1310 nm lasers for the CMS Tracker optical links, IEEE Trans. Nucl. Sci. 49 (6) (2002) 2923–2929, http://dx.doi.org/10.1109/TNS.2002.805422.

[17] I. Dawson (Ed.), Radiation Effects in the LHC Experiments, CERN, 2021, http://dx.doi.org/10.23731/CYRM-2021-001.

[18] F. Faccio, P. Moreira, A. Marchioro, 80-Mbit/s radiation-tolerant optical receiver for the CMS digital optical link, in: E.W. Taylor (Ed.), in: Photonics for Space Environments VII, vol. 4134, SPIE, International Society for Optics and Photonics, 2000, pp. 185–193, http://dx.doi.org/10.1117/12.405343.

[19] D. Charlton, et al., Radiation hardness and lifetime studies of photodiodes for the optical readout of the ATLAS semiconductor tracker, Nucl. Instrum. Methods Phys. Res. A 456 (3) (2001) 300–309, http://dx.doi.org/10.1016/S0168-9002(00)00666-5.

[20] K. Gill, M. Axer, S. Dris, R. Grabit, R. Macias, E. Noah, J. Troska, F. Vasey, Radiation hardness assurance and reliability testing of ingaas photodiodes for optical control links for the CMS experiment, IEEE Trans. Nucl. Sci. 52 (5) (2005) 1480–1487, http://dx.doi.org/10.1109/TNS.2005.855811.

[21] G. Mahout, et al., Irradiation studies of multimode optical fibres for use in ATLAS front-end links, Nucl. Instrum. Methods Phys. Res. A 446 (3) (2000) 426–434, http://dx.doi.org/10.1016/S0168-9002(99)01275-9.

[22] M. Chu, et al., The off-detector opto-electronics for the optical links of the ATLAS semiconductor tracker and pixel detector, Nucl. Instrum. Methods Phys. Res. A 530 (3) (2004) 293–310, http://dx.doi.org/10.1016/j.nima.2004.04.228.

[23] F. Vasey, C. Biber, M. Sugiyama, J. Troska, A 12-channel analog optical-receiver module, J. Lightwave Technol. 23 (12) (2005) 4270–4277, http://dx.doi.org/10.1109/JLT.2005.858226.

[24] A.R. Weidberg, VCSEL reliability in ATLAS and development of robust arrays, J. Instrum. 7 (7) (2012) C01098, http://dx.doi.org/10.1088/1748-0221/7/01/C01098.

[25] K. Gan, P. Buchholz, S. Che, R. Ishmukhametov, H. Kagan, R. Kass, K. Looper, J. Moore, J. Moss, D. Smith, Y. Yang, M. Ziolkowski, Design, production, and reliability of the new ATLAS pixel opto-boards, J. Instrum. 10 (02) (2015) C02018, http://dx.doi.org/10.1088/1748-0221/10/02/c02018.

[26] The LHCb Outer Tracker group, Performance of the LHCb outer tracker, J. Instrum. 9 (01) (2014) P01002, http://dx.doi.org/10.1088/1748-0221/9/01/p01002.

[27] Joint ATLAS-CMS working group on opto- electronics for SLHC report from sub-group A: Lessons learned and to be learned from LHC, 2007, URL https://edms.cern.ch/document/882775/3.8.

[28] B. Allongue, S. Buso, G. Blanchot, F. Faccio, C. Fuentes, P. Mattavelli, S. Michelis, S. Orlandi, G. Spiazzi, Custom DC-DC converters for distributing power in SLHC trackers, in: Proceedings of the Topical Workshop on Electronics for Particle Physics, TWEPP-2008, Naxos, Greece, 2008, pp. 289–293, CERN/LHCC/2008-008.

[29] J. Troska, S. Detraz, S. Papadopoulos, I. Papakonstantinou, S. Rui Silva, S. Seif el Nasr, C. Sigaud, P. Stejskal, C. Soos, F. Vasey, The Versatile Transceiver Proof of Concept, in: Proceedings of the Topical Workshop on Electronics for Particle Physics, TWEPP-2008, Naxos, Greece, 2009, pp. 347–351, CERN/LHCC/2009-006.

[30] F. Vasey, D. Hall, T. Huffman, S. Kwan, A. Prosser, C. Soos, J. Troska, T. Weidberg, A. Xiang, J. Ye, The Versatile Link common project: Feasibility report, J. Instrum. 7 (01) (2012) C01075, URL http://stacks.iop.org/1748-0221/7/i=01/a=C01075.

[31] J. Troska, A. Brandon-Bravo, S. Detraz, A. Kraxner, L. Olanterä, C. Scarcella, C. Sigaud, C. Soos, F. Vasey, The VTRx+, an optical link module for data transmission at HL-LHC, Proc. Sci. 313 (2017) 048, http://dx.doi.org/10.22323/1.313.0048, URL https://pos.sissa.it/313/048.

[32] P. Moreira, K. Wyllie, A. Marchioro, C. Paillard, J. Li, S. Bonacini, F. Faccio, D. Porret, S. Baron, P. Gui, R. Francisco, O. Cobanoglu, S. Feger, The GBT-SerDes ASIC prototype, J. Instrum. 5 (2010) C11022, URL https://cds.cern.ch/record/1359272.

[33] GBT project web site, 2020, URL https://espace.cern.ch/GBT-Project.

[34] Small Form Factor Committee, SFF-8431 specifications for enhanced small form factor pluggable module SFP+, 2009, URL https://www.10gtek.com/templates/wzten/pdf/SFF-8431-(SFP+%20MSA).pdf.

[35] Z. Zeng, T. Zhang, G. Wang, P. Gui, S. Kulis, P. Moreira, LDQ10: A compact ultra low-power radiation-hard 4 × 10 Gb/s driver array, J. Instrum. 12 (02) (2017) P02020, http://dx.doi.org/10.1088/1748-0221/12/02/p02020.

[36] M. Menouni, P. Gui, P. Moreira, The GBTIA, a 5 Gbit/s radiation-hard optical receiver for the SLHC upgrades, 2009, Topical Workshop on Electronics for Particle Physics (TWEPP2009). URL http://cdsweb.cern.ch/record/1185010.

[37] S.F.F. Committee, SFF-8436: QSFP+ 4X 10 Gb/s pluggable transceiver, 2015, URL http://www.snia.org/sff/specifications.

[38] G. Cummings, on behalf of the CMS Collaboration, CMS HCAL VTRx-induced communication loss and mitigation, J. Instrum. 17 (05) (2022) C05020, URL https://doi.org/10.1088/1748-0221/17/05/C05020.

[39] D. Hall, B.T. Huffman, A. Weidberg, The radiation induced attenuation of optical fibres below -20 °C exposed to lifetime HL-LHC doses at a dose rate of 700 Gy(Si)/hr, J. Instrum. 7 (01) (2012) C01047, URL http://stacks.iop.org/1748-0221/7/i=01/a=C01047.

[40] B.T. Huffman, A. Weidberg, Summary of the effects of radiation upon the passive optical components of the Versatile Link, J. Instrum. 9 (01) (2014) C01018, URL http://stacks.iop.org/1748-0221/9/i=01/a=C01018.

[41] J. Blanc, F. Achten, A. Alessi, A. Amezcua, J. Kuhnhenn, A. Pastouret, D. Ricci, I. Toccafondo, Characterization of radiation-resistant multimode optical fibers for large-scale procurement, IEEE Trans. Nucl. Sci. 68 (7) (2021) 1407–1413, http://dx.doi.org/10.1109/TNS.2021.3074633.

[42] Versatile Link Plus Project Team, Versatile link plus technical specification, part 1: System, 2019, URL https://edms.cern.ch/document/1719328/1.

[43] Intel, AN 835: PAM4 signaling fundamentals, 2019, URL https://www.intel.com/content/www/us/en/docs/programmable/683852/current/introduction.html.

[44] S. Seif El Nasr-Storey, Radiation-hard Optoelectronics for LHC detector upgrades. (Ph.D. thesis), Bristol U., 2016-06-22, URL http://inspirehep.net/record/1503530/files/CERN-THESIS-2016-141.pdf.

[45] S. Papadopoulos, S.S.E. Nasr-Storey, J. Troska, I. Papakonstantinou, F. Vasey, I. Darwazeh, Component and system level studies of radiation damage impact on reflective electroabsorption modulators for use in HL-LHC data transmission, IEEE Trans. Nucl. Sci. 60 (1) (2013) 386–393, http://dx.doi.org/10.1109/TNS.2012.2231964.

[46] D. Thomson, A. Zilkie, J.E. Bowers, T. Komljenovic, G.T. Reed, L. Vivien, D. Marris-Morini, E. Cassan, L. Virot, J.-M. Fédéli, J.-M. Hartmann, J.H. Schmid, D.-X. Xu, F. Boeuf, P. O'Brien, G.Z. Mashanovich, M. Nedeljkovic, Roadmap on silicon photonics, J. Opt. 18 (7) (2016) 073003, http://dx.doi.org/10.1088/2040-8978/18/7/073003.

[47] S.S.E. Nasr-Storey, F. Boeuf, C. Baudot, S. Detraz, J.M. Fedeli, D. Marris-Morini, L. Olanterä, G. Pezzullo, C. Sigaud, C. Soos, J. Troska, F. Vasey, L. Vivien, M. Zeiler, M. Ziebell, Effect of radiation on a Mach-Zehnder interferometer silicon modulator for HL-LHC data transmission applications, IEEE Trans. Nucl. Sci. 62 (1) (2015) 329–335, http://dx.doi.org/10.1109/TNS.2015.2388546.

[48] M. Zeiler, S. Detraz, L. Olanterä, C. Sigaud, C. Soos, J. Troska, F. Vasey, A system-level model for high-speed, radiation-hard optical links in HEP experiments based on silicon Mach-Zehnder modulators, J. Instrum. 11 (12) (2016) C12059, URL http://stacks.iop.org/1748-0221/11/i=12/a=C12059.

[49] M. Lalović, C. Scarcella, A. Bulling, S. Detraz, L. Marcon, L. Olanterä, T. Prousalidi, U. Sandven, C. Sigaud, C. Soos, J. Troska, Ionizing radiation effects in silicon photonics modulators, IEEE Trans. Nucl. Sci. 69 (7) (2022) 1521–1526, http://dx.doi.org/10.1109/TNS.2022.3148579.

[50] T. Prousalidi, A. Bulling, M. Court, S. Detraz, M. Lalović, L. Marcon, L. Olanterä, S. Orfanelli, U. Sandven, C. Scarcella, C. Sigaud, C. Soós, J. Troska, Towards optical data transmission for high energy physics using silicon photonics, J. Instrum. 17 (05) (2022) C05004, http://dx.doi.org/10.1088/1748-0221/17/05/c05004.

[51] F. Poletti, M.N. Petrovich, D.J. Richardson, Hollow-core photonic bandgap fibers: Technology and applications, Nanophotonics 2 (5–6) (2013) 315–340, http://dx.doi.org/10.1515/nanoph-2013-0042.

[52] L. Olanterä, C. Sigaud, J. Troska, F. Vasey, M.N. Petrovich, F. Poletti, N.V. Wheeler, J.P. Wooler, D.J. Richardson, Gamma irradiation of minimal latency hollow-core photonic bandgap fibres, J. Instrum. 8 (12) (2013) C12010, http://dx.doi.org/10.1088/1748-0221/8/12/c12010.

[53] P. Poggiolini, F. Poletti, Opportunities and challenges for long-distance transmission in hollow-core fibres, J. Lightwave Technol. 40 (6) (2022) 1605–1616, http://dx.doi.org/10.1109/JLT.2021.3140114.

[54] IEEE Standard for Ethernet – Amendment 7: Physical Layer and Management Parameters for 400 Gb/s over Multimode Fiber, 2020, pp. 1–72, http://dx.doi.org/10.1109/IEEESTD.2020.9052826, IEEE Std 802.3cm-2020 (Amendment To IEEE Std 802.3-2018 As Amended By IEEE Std 802.3cb-2018, IEEE Std 802.3bt-2018, IEEE Std 802.3cd-2018, IEEE Std 802.3cn-2019, IEEE Std 802.3cg-2019, and IEEE Std 802.3cq-2020).

[55] M. Aleksa, J. Blomer, B. Cure, M. Campbell, C. D'Ambrosio, D. Dannheim, M. Doser, F. Faccio, P. Farthouat, C. Gargiulo, P. Janot, C. Joram, M. Krammer, L. Linssen, P. Mato Vila, P. Rodrigues Simoes Moreira, L. Musa, E. Oliveri, A. Onnela, H. Pernegger, P. Riedler, C. Rembser, G. Stewart, H. Ten Kate, F. Vasey, Strategic R&D Programme on Technologies for Future Experiments, Tech. Rep., CERN, Geneva, 2018, URL https://cds.cern.ch/record/2649646.

[56] S. Cammarata, P. Velha, F. Di Pasquale, S. Saponara, F. Palla, S. Faralli, Silicon photonic devices for optical data readout in high-energy physics detectors, Nucl. Instrum. Methods Phys. Res. A 1045 (2023) 167576, http://dx.doi.org/10.1016/j.nima.2022.167576.